

OMAE2008-57440

Serviço de Bibliotecas  
Biblioteca de Engenharia Mecânica, Naval e Oceânica

## CONCEPTUAL DESIGN OF FLOATING PRODUCTION AND STORAGE WITH DRY TREE CAPABILITY

Rodolfo Trentin Gonçalves<sup>1</sup>  
([rodolfo\\_tg@tpn.usp.br](mailto:rodolfo_tg@tpn.usp.br))

Fabio Tadao Matsumoto<sup>1</sup>  
([fabio\\_matsumoto@tpn.usp.br](mailto:fabio_matsumoto@tpn.usp.br))

Higor Felipe de Medeiros<sup>1</sup>  
([higorfm@gmail.com](mailto:higorfm@gmail.com))

Hernani Luiz Brinati<sup>1</sup>  
([hbrinat@usp.br](mailto:hbrinat@usp.br))

Kazuo Nishimoto<sup>1</sup>  
([knishimo@usp.br](mailto:knishimo@usp.br))

Isaías Quaresma Masetti<sup>2</sup>  
([masetti@petrobras.com.br](mailto:masetti@petrobras.com.br))

<sup>1</sup> Department of Naval Architecture and Ocean Engineering  
Escola Politécnica – University of São Paulo  
São Paulo, SP, Brazil

<sup>2</sup> Research and Development Center (CENPES)  
PETROBRAS  
Rio de Janeiro, RJ, Brazil

### ABSTRACT

This paper introduces a new concept and a preliminary study for a floating unit aimed at exploring and producing oil in ultra deep waters. This platform, which combines two relevant features - great oil storage capacity and dry tree production capability - comprises two bodies with relatively independent heave motions between them. A parametric model is used to define the main design characteristics of the floating units. A set of design alternatives is generated using this procedure. These solutions are evaluated in terms of stability requirements and dynamic response. A mathematical model is developed to estimate the first order heave and pitch motions of the platform. Experimental tests are carried out in order to calibrate this model. The response of each body alone is estimated numerically using WAMIT<sup>®</sup> code. The paper also includes a preliminary study of the platform mooring system.

### 1. INTRODUCTION

In recent years, Brazil has been beating water depth records in offshore oil exploration, with new reserves of oil and gas having been discovered and confirmed by Petrobras. This scenario leads the oil industry to develop and modernize itself in order to meet the huge market demand. A continuing

challenge for the industry is to reduce production costs in areas of ultra deep water.

In this context, a new concept of a floating unit for exploration and production of oil in ultra deep waters is proposed. This concept provides great storage capacity and dry tree production capability. Both characteristics aim to reduce the costs of oil production. In order to obtain dry completion, reduced motions of the intervention system are required. A similar concept to meet these requirements was proposed by Poldervaart L. & Pollack J. [10].

This concept comprises two bodies, with relatively independent heave motions between them, where one body (mono-column with moonpool) works as a storage unit and the other one as a dry completion unit located inside the moonpool. The concept's feasibility, with high storage capability and reduced motion, is also discussed. Details about the mono-column concept are presented in Cueva, M. [13].

This paper's next section – Design Conception – presents the design premises as well as the main characteristics of the new concept. It is followed by a section which presents a description of the model's tests and the numeric models used to describe the platform's response, as well as the calibration of the numeric model based on the experimental results.

Subsequently, the Design Procedure section presents the philosophy used to design the platform. The last section presents the conclusions regarding the feasibility of the New Concept.

## 2. DESIGN CONCEPTION

In this section, the design premises and the main features of the New Concept are outlined.

**New Concept:** The New Concept, illustrated in Figure 1, is characterized by the presence of two bodies.

The Main Body is similar to a mono-column platform with a moonpool. The Main Body has the following functions:

- Production storage;
- Supporting the process plant, intervention tower and living quarters;
- The mooring lines are fixed to the Main Body. Due to offset limitation, the mooring lines system has a taut-leg configuration.

The Inner Body, which is inside the Main Body moonpool, has the following functions:

- Supporting the dry tree;
- Connection of the risers system. The risers are TTR configuration (top tension riser). Pre-tension of the risers are provided by the Inner Body buoyancy.

The two bodies need to have relatively independent vertical motions. This motion decoupling is provided by a rolling system, which allows a free vertical motion of the Inner Body inside the Main Body moonpool.

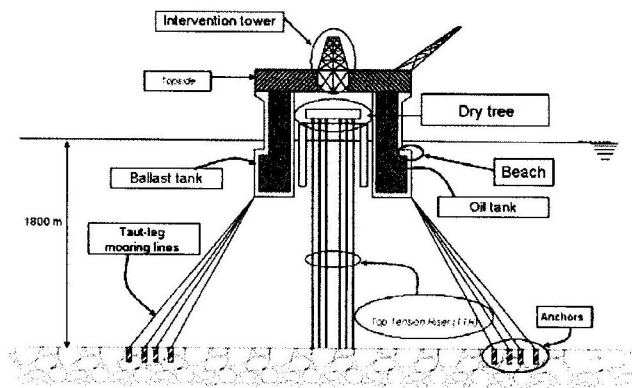


Figure 1 - Schematic of the New Concept.

**Design Basis:** The design basis for the New Concept is as follows:

- Campos Basin (Brazil) environment;
- Ultra deep water;
- Storage capacity;
- 8 radial tanks;
- 9 risers (11 ¾ in OD and wall thickness 1 ¼ in);

- Spacing between the moonpool walls and the Inner Body external side: 3m, which is assumed wide enough to accommodate the rolling system;
- Moonpool diameter large enough to support the deck area for the dry tree;
- Taut-leg mooring lines are required due to the limited offset allowed (5% of water depth);
- 70 per cent or more of the operation time in fixed ballast condition.

**Environment:** The environment conditions are typical of the Campos Basin in Brazil.

Three wave spectra have been assumed to correspond respectively to 1, 10 and 100 year sea levels.

- Sea 1: JONSWAP spectrum  $\gamma=1.76$ ,  $H_s=6.37\text{m}$ ,  $T_p=13.93\text{s}$ ;
- Sea 2: JONSWAP spectrum  $\gamma=1.71$ ,  $H_s=7.16\text{m}$ ,  $T_p=14.78\text{s}$ ;
- Sea 3: JONSWAP spectrum  $\gamma=1.66$ ,  $H_s=7.84\text{m}$ ,  $T_p=15.55\text{s}$ .

A water depth equal to 1,800m is assumed.

**Risers system:** The steel risers are TTR. It is assumed that a Heave motion compensation system is not required.

TTR risers should not be compressed; therefore they must be pre-tensioned. Pre-tension of risers are provided by the buoyancy of the Inner Body. If required, tension on risers could be modified, either by applying tensors on the risers' extremities or by performing a ballast operation of the Inner Body.

Pre-tension was calculated for 1.6m vertical displacement. The result is a pre-tension equal to a 256.8 ton/riser.

**Hull dimensions:** The Main Body is similar to a mono-column with a moon pool, and is designed in such a way that its beach is always below the water line for the different loading conditions. The moonpool has parallel walls to accommodate the Inner Body in its interior. The Main Body is double sided and follows the rules of MARPOL 73/78 [1].

The Inner Body is cylindrical and has ballast tanks. The buoyancy of the Inner Body should support the dry tree weight and the risers' pre-tension.

**Mooring system:** The Mooring lines present taut-leg configuration due to limited offset. The line consists of a 50m segment of #4 bottom chain, a 50m top spiral strand segment and a polyester segment with a post-evaluated length. The polyester segment is calculated according to the layout of the mooring system (number and angles of the lines).

## 3. MODEL TESTS AND NUMERICAL CALIBRATION

### Model test

**General description:** The test matrix was accomplished at the Department of Naval Architecture and Ocean Engineering basin, at the University of São Paulo in July 2007. The model scale was 1:150. The models are shown in Figure 2. The prototype dimensions for the Main Body and the Inner Body are presented in Figure 3 and 4, respectively.

The experiments were carried out in regular waves and in transient waves; there were also decay tests in Heave and Pitch motions. The tests were made with and without the Inner Body inside the Main Body moonpool, in order to investigate the influence of the Main Body on the Inner Body response.

All the tests in waves were carried out without the presence of mooring lines or risers

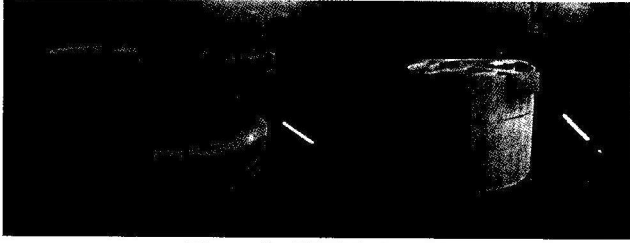


Figure 2 - Models to scale

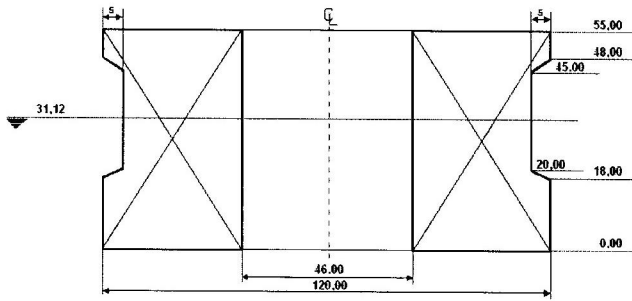


Figure 3 - Prototype dimensions - Main Body

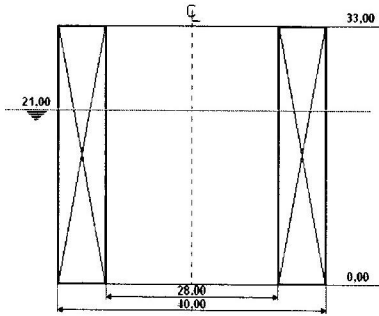


Figure 4 - Prototype dimensions - Inner Body

Three different platform configurations were considered in the tests:

- SS1: The Main Body alone;
- CI1: The Inner Body alone;
- SS2: The Main Body and Inner Body together.

Figure 5 shows the settings for configuration SS2.

#### Results highlights

**Natural periods:** The natural periods, derived from the decay tests, are shown in Table 1 and Table 2, for Heave and

Pitch motion, respectively. The decay tests were performed without risers or mooring lines.

The results show that the Main Body natural periods do not change in the presence of the Inner Body. The Heave natural period of the Inner Body changes in the presence of the Main Body, due to the fluid flow between them.

**First order motions:** The first order motions were evaluated through the RAO (response amplitude operator) obtained from the model test submitted to waves.

The experimental results are presented along with the numerical RAO for comparison purposes in Figure 7 to 9.

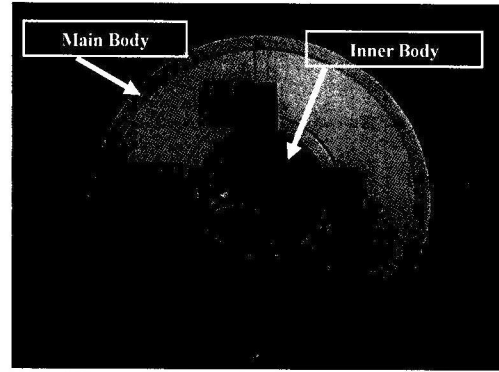


Figure 5 - Experimental setup – SS2

#### Numerical versus model tests

**General:** The numerical model used in this paper was suggested by Torres, F. [11] and Malta, E. B. [12], and was developed using WAMIT® code [3]. WAMIT® code applies potential theory to evaluate the motions of each body separately.

Figure 6 shows a mesh example of the model.

To evaluate the Inner Body dynamics in the presence of the main body, the following formulation was used:

$$RAO_{Inner}^*(\omega) = RAO_{Moonpool}(\omega) \cdot RAO_{Inner}(\omega) \quad (1)$$

where:

$RAO_{Inner}^*$  is the Inner Body RAO in the presence of the Main Body;

$RAO_{Moonpool}$  is the free surface elevation at the Main Body moonpool;

$RAO_{Inner}$  is the Inner Body RAO alone;

$\omega$  is the frequency wave.

This formulation assumes that the Inner Body is excited by the elevation of the Main Body moonpool and the free surface is not disturbed by the Inner Body.

The numerical models are calibrated based on the experimental results.

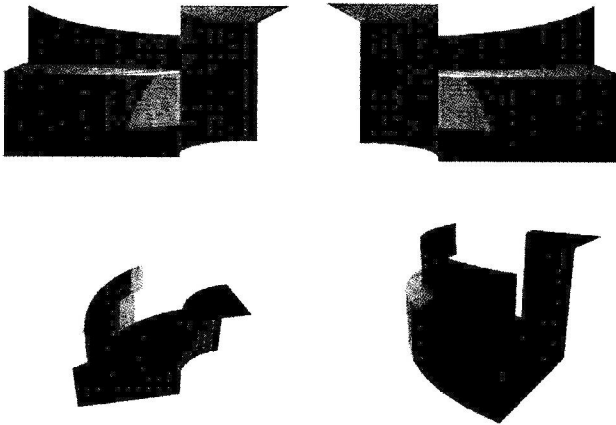


Figure 6 - Mesh of the Main Body

**Result highlights:** The numerical and the experimental RAO are presented below. The full lines represent the numerical results and the dashed lines the experimental ones.

Figure 7 illustrates the RAO comparison for the Main Body heave motion without the Inner Body while Figure 8 illustrates the comparison for the heave motion of the Inner Body alone.

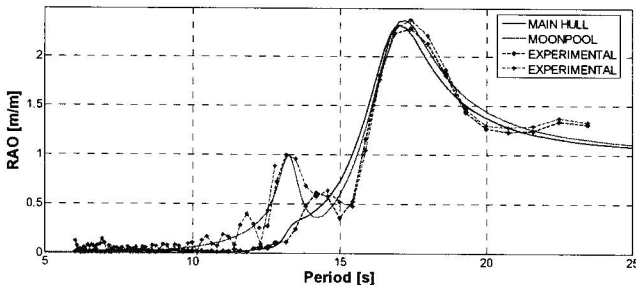


Figure 7 - Comparison of Heave motion RAO- Main Body

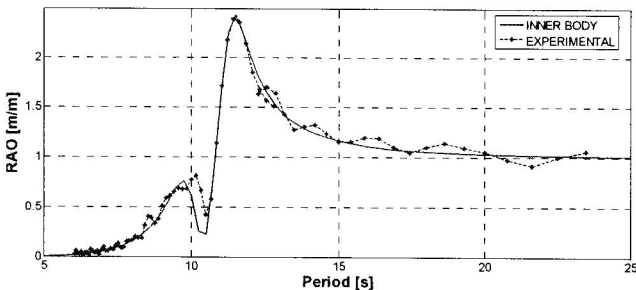


Figure 8 - Comparison of Heave motion RAO - Inner Body

Figure 9 shows the comparison between numerical and experimental results for the heave motion of the Inner Body in the presence of the Main Body. The numerical results in this case were obtained by using Equation 1.

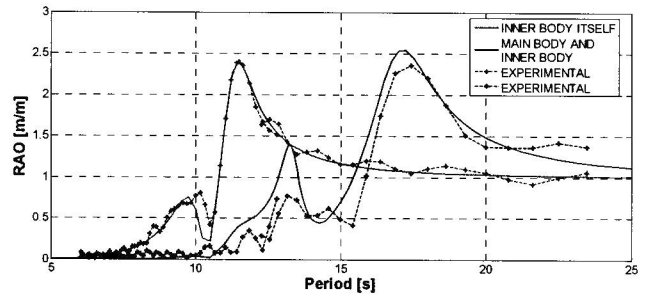


Figure 9 - Comparison of Heave motion RAO - Inner Body with Main Body

**Conclusion:** It can be seen that there is a good agreement between the experimental results and the calibrated numerical ones. Therefore, the proposed model equation (1) will be used to evaluate the Inner Body dynamics inside the Main Body.

#### 4. DESIGN PROCEDURE

The methodology adopted to develop the preliminary design of the new system concept is presented in this section, considering its operation in Brazilian offshore oil fields.

##### Design-general requirements

- Brazilian environment;
- Storage capacity: 800,000 BBLs;
- Topsides capacity: 100,000 Bopd.

##### Design environmental conditions

A water depth of 1,800m is assumed.

The centenary sea spectrum is used to develop the system design; nevertheless, the system performance is also investigated in two water conditions, as was previously mentioned. The parameters of these conditions are defined in Table 3.

The wind and current characteristics are shown in Tables 4 and 5, respectively.

##### Hull design

A parametric model, which takes into account the design premises and requirements, was used to generate different hull alternatives.

The parametric model has as its main feature the division of the platform in slices as illustrated in Figure 10. The evaluation of the system characteristics is performed for each slice individually and, afterwards, the results are integrated to provide the characteristics of the entire system.





### Figure 11 - Design variables

- $GM > 1.0m$ ;
- $R_{int} > 23.0m$ , in order to provide dry tree production capability;
- $Dp_{max} < 20.0m$ , related to the minimum draft of the Main Body, in order to avoid hawser disconnection;
- $Dp_{min} > 8.0m$ , related to the maximum draft of the Main Body, to avoid shock between the two bodies;
- Loading conditions for maximum and minimum draft, which meet a system operation period greater than 70 per cent in fixed ballast.

The evaluation of hull mass and inertia takes into account the structural mass (computed from the model presented by Malta E. B. [2]), as well as oil and ballast; the two last components depend on the loading condition.

The main characteristics of the three design alternatives are presented in Table 6. The main dimensions of the C03 alternative are presented in Figure 12.

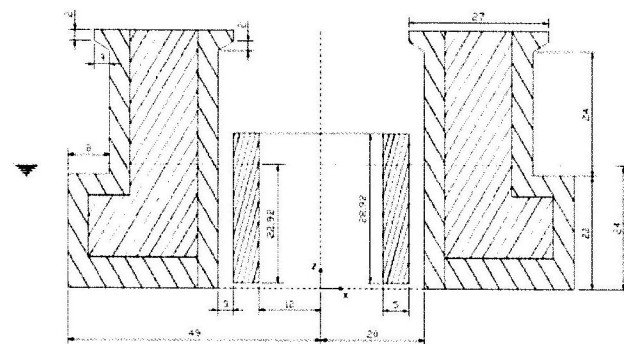


**Figure 12 - Main dimensions - C03**

The stability results are illustrated in table 8 and indicate that the CO2 alternative does not satisfy the damage stability criteria; therefore, this alternative will not be considered in the next design stages.

The RAOs results for the Heave motion of the Main Body are illustrated in Figure 13. The RAOs results for the Pitch motion of the Main Body are illustrated in Figure 14. The RAOs results for the Heave motion of the Inner Body taking into consideration restoring forces due to the risers are illustrated in Figure 15. The blue lines identify the C01 Alternative results and the red lines the C03's.

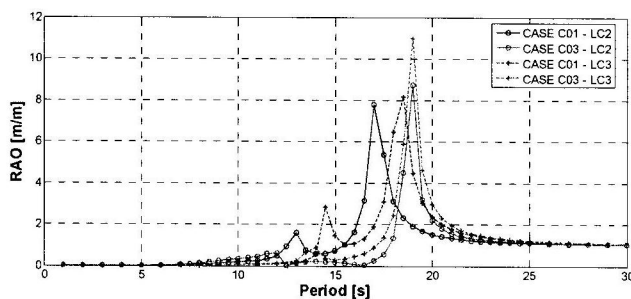


**Figure 13 - Heave motion RAOs - Main Body**

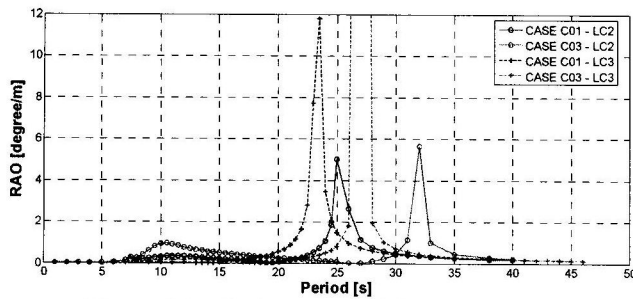


Figure 14 – Pitch motion RAOs – Main Body

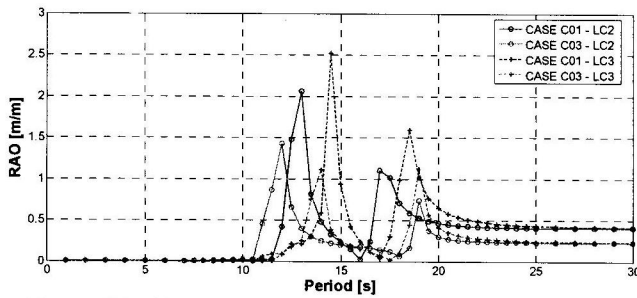


Figure 15 - Heave motion RAOs - Inner body with risers, restoring forces

It should be pointed out that the results were obtained without taking into consideration the viscous damping since only the potential component was included in the model.

The RAO results were used to obtain the significant height for Heave and Pitch motions. The significant height was calculated by:

$$H_s = 4 \cdot \sqrt{m_0} \quad (2)$$

where

$$m_0 = \int_0^\infty S_R(\omega) d\omega \quad (3)$$

$$S_R(\omega) = S_w(\omega) \cdot RAO^2(\omega) \quad (4)$$

where:

$m_0$  is the zero order moment of the response spectrum;

$S_R$  is the response spectrum;

$S_w$  is the wave spectrum obtained by the Jonswap formulation.

Tables 9 and 11 illustrate the results of significant heights for the Heave motion of the Main Body and the Inner Body, respectively. The results were obtained in the frequency domain considering only the potential damping.

Table 10 illustrates the significant height result for the Pitch motion of the Main Body. The C03 Alternative has a better performance than C01's in first order Heave motion

(lower significant heights) in all loading conditions. In the case of the Pitch motion, the alternative C03 has also a better performance; only in the LC2 loading condition does the C01 exhibit a smaller significant height.

As the alternative C03 has shown a better performance, further analysis of motion response was performed with this configuration. The evaluation of the system motion for the C03 alternative was performed for three different levels of viscous damping for the Heave and Pitch motion of the Main Body:  $\zeta=2\%$ ,  $\zeta=4\%$  and  $\zeta=6\%$ ; the RAOs results are presented in Figures 16 to 18. The viscous damping for the free surface elevation was assumed to be equal to 2%; based on previous experimental results, a viscous damping equal to 6% for the heave motion of the Inner Body was assumed.

Tables 12 and 14 illustrate the results of significant height for the Heave motion of the Main Body and the Inner Body, respectively, considering the different levels of viscous damping. It is expected that the incorporation of the viscous damping leads to results closer to the experimental ones.

The results for the Pitch motion are illustrated in Table 13. There was no difference between the results for the different levels of damping because the natural period of Pitch is far from the wave spectrum peak. The Pitch motion response in the loading condition LC2 is considered large when compared to the response of similar units.

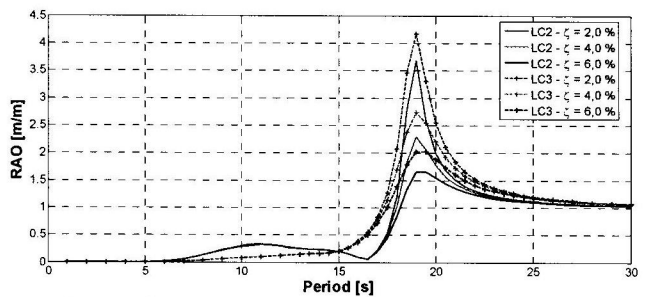


Figure 16 – Heave motion RAOs – Including viscous damping – Main Body

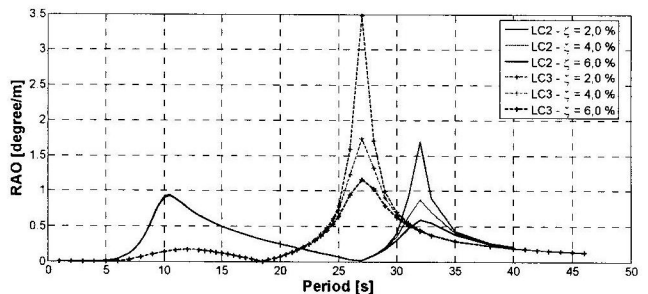
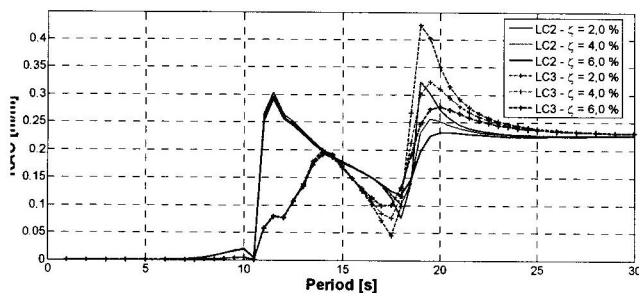


Figure 17 – Pitch motion RAOs – Including viscous damping – Main Body



**Figure 18 – Heave motion RAOs – Including viscous damping – Inner Body**

The heave motion of the Inner Body is relevant since it will determine tensions acting upon the risers. Since each point on the deck of the Inner Body presents a different motion, the deck surface was discretized and the acceleration of the coupled motion (Heave and Pitch) of each point was evaluated.

The results for the Alternative C03 in the loading condition LC2, for  $\zeta=2\%$ , are illustrated in Figure 19 as a function of gravity acceleration. Since an acceleration equal to 10% of the gravity acceleration is considered acceptable as good machinery performance and since the results obtained are lower than this, the system performance is satisfactory.

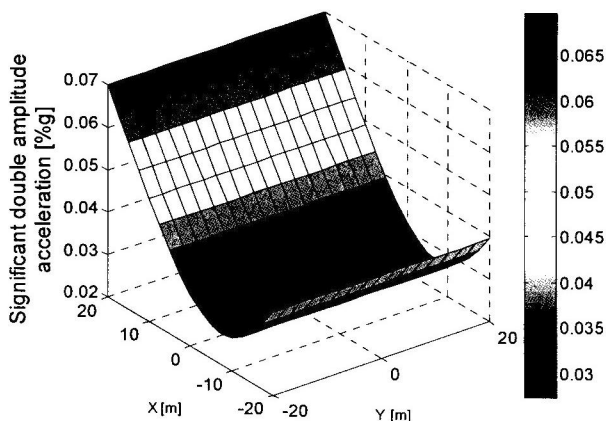


**Figure 19 – Significant double amplitude acceleration at deck of Inner Body - Case C03 - Loading condition LC2**

The relative motion between the two bodies is important for the system's safety because a high relative motion may cause a collision between two decks or a disconnection of the oil hoses.

The results for relative motions for the alternative C03 are illustrated in Table 15. Only in case of the loading condition LC2 and viscous damping  $\zeta=2\%$  the relative motion exceeds 8.0 m, which will cause a shock between the two bodies. However, the damping coefficient considered ( $\zeta=2\%$ ) is lower than the damping measured in similar units.

### Low frequency Surge motion

The Main Body second order motion of Surge is important in order to design the mooring system, because its performance will depend on the system offset.

The offset of the New Concept should be small due to the dry completion requirement, which cannot support high tensions. Another problem created by high offsets is the Inner Body sinkage, which will cause the disconnection of the hoses.

The RMS of the second order motion of Surge, using a damping  $\zeta=2\%$ , was evaluated according to Aranha J.P. [6]. The second order forces were estimated using WAMIT® code.

Figure 20 illustrates the RMS results of the second order surge motion for the alternatives C01 and C03 in the survivability conditions of the Campos Basin. The results are given for different stiffness of the mooring system.

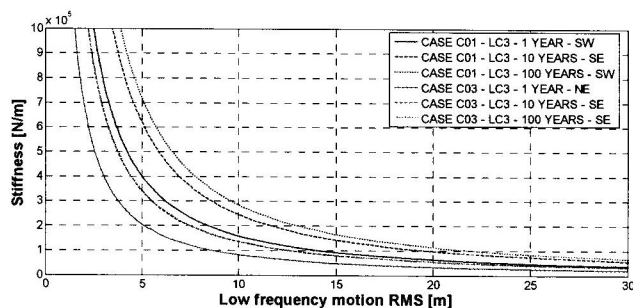


**Figure 20 –Low frequency motion RMS**

### Design of the Mooring System

The design takes into consideration the different compositions of the mooring lines. The lines, as previously mentioned, are composed of three parts:

- Lower end: 50 m #4 chain;
- Upper end: 50 m of spiral strand;
- Intermediate part: polyester.

A design procedure proposed by Martin; M.R. [7] and [8] was used; the force evaluation and the adopted design criteria are based on the DNV rules [9].

The length of the intermediate part of the mooring line, the maximum tension on the lines, the maximum offset, and the anchorage radius were evaluated for a given configuration of the mooring lines in such a way that the mooring system satisfied the design requirements:

- Taut-leg system, thus the length of the line part supported on the sea floor equals zero;
- Maximum offset equals 10% of water depth;
- Maximum allowable tension acting on the lines equal 55.6 % of the ultimate strength.

The design environmental condition is defined as the survivability condition, according to the DNV norm. Figure 21 illustrates the forces applied to the platforms for Alternative C03 due to the environmental agents (wind, wave and current).

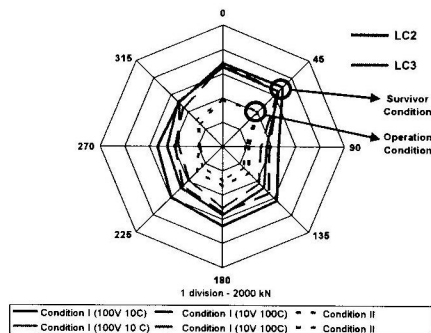


Figure 21 – Static forces on Case C03

Different values of the damping coefficient for the Surge motion, as shown in Figure 22, were used to evaluate the performance of the mooring system. A change in the damping coefficient leads to a change in the RMS of the second order Surge motion.

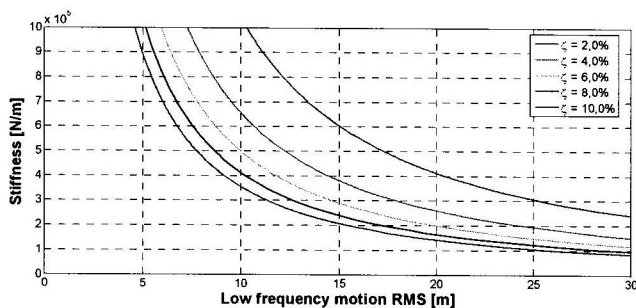


Figure 22 - Different damping coefficients on low frequency surge motion

The line configurations considered to perform the design of the mooring system are illustrated in Figure 23.

A set of feasible solutions provided by the design procedure for the above lines configuration, is presented in Figure 24 for a damping coefficient  $\zeta=2\%$ . These solutions are presented in an offset[m] versus anchorage radius[m] graphic.

It can be seen that the offsets in the level of 5% of the water depth are obtained with the adopted configurations, which means there is a good margin of safety in respect to the specified requirement.

### Conclusions

A design procedure for the new floating concept was proposed based on a parametric model; three different alternatives were generated considering main design criteria.

The stability analysis indicated that one of these alternatives (C02) did not meet the static stability requirements specified by the ABS rules.

The study of system dynamic behavior, considering first and second order responses in Heave and Pitch motions indicated that the alternative C03 had a better performance than the C01's.

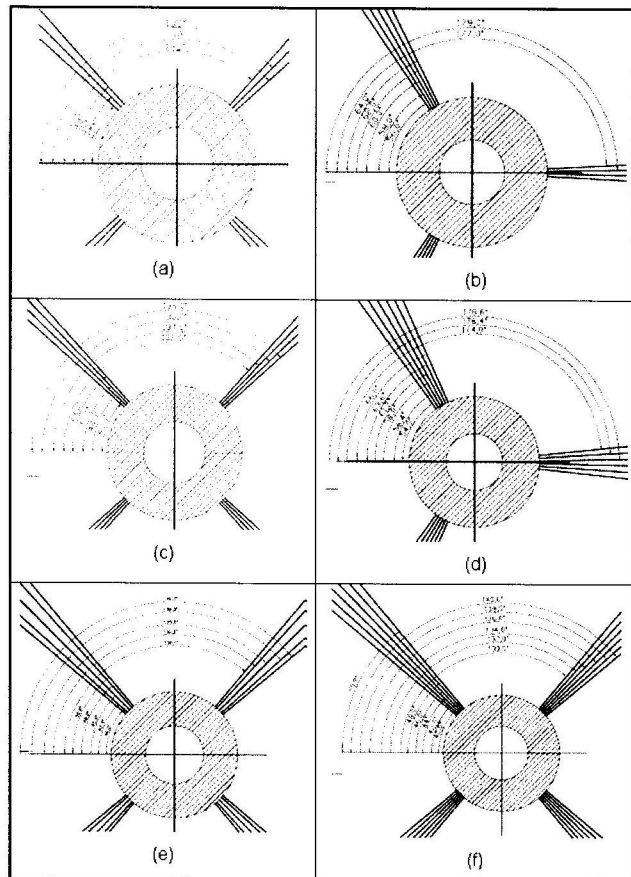


Figure 23 - Mooring line layout (a) 12 lines (b) 14 lines (c) 16 lines (d) 18 lines (e) 20 lines (f) 24 lines

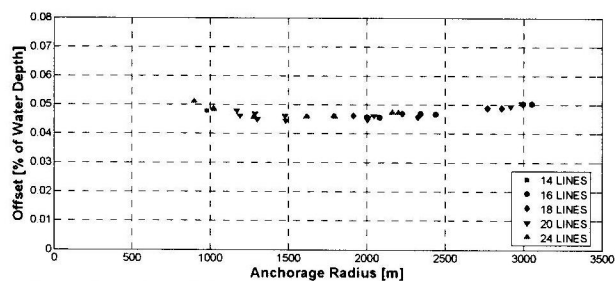


Figure 24 – Feasible solutions of mooring systems -  $\zeta=2\%$

For the best alternative (C03), further analysis of the first order motions was performed considering the incorporation of realistic viscous damping; the system response was improved.

The final results showed that the first order motion, mainly the pitch, must be improved. This improvement can be obtained by incorporating hydrodynamic appendices (Heave plate) as proposed by Thiagarajan, K. P. & Troesch, A. W. [14] and Tao, L. & Cai, S. [15], with the purposes of increasing the added mass and the viscous damping.

Finally, the design of the mooring system employed for the best alternative (C03), and its results demonstrated the feasibility of the concept, considering 5% of water depth the maximum offset.

## 5. GENERAL CONCLUSIONS

The new concept of a floating production and storage system with dry tree capability can be considered feasible according to the studies presented in this paper.

A detailed study of the body motions and static stability is presented as well, including a parametric model to generate the platform characteristics. A set of model tests were carried out to validate the numerical models, showing a good agreement between the results.

However, to consolidate this concept, new studies should be carried out. For instance, the second order motion of the platform should be used in the estimation for the first order motion as it will influence the relative motion between the two bodies.

The entire platform may be optimized, for instance, with the inclusion of hydrodynamic appendices in the Main Body and changes in the Inner Body geometry.

This paper should be considered as a starting point for further studies of this new conception.

## NOMENCLATURE

$\gamma$	Peakedness parameter
$\omega$	Wave frequency [rad/s]
$\zeta$	Damping coefficient
$BL_s$	Inner Body freeboard [m]
C02	Case Id C02
C03	Case Id C03
D	Depth [m]
Dc	Double side [m]
Df	Double bottom [m]
Dp	Difference between decks [m]
Dp <sub>max</sub>	Maximum difference between decks [m]
Dp <sub>min</sub>	Minimum difference between decks [m]
GM	Metacentric height [m]
GZ	Righting moment curve
H <sub>praia</sub>	Main Body beach height [m]
H <sub>s</sub>	Significant height [m]
LC2	Loading condition LC2 (minimum draft) [m]
LC3	Loading condition LC3 (maximum draft) [m]
L <sub>praia</sub>	Main Body beach width [m]
Lt	Inner Body ballast tank width [m]
m <sub>0</sub>	Zero order moment of spectrum [m <sup>2</sup> ]
RAO	Response amplitude operator
RAO <sub>Moonpool</sub>	Moonpool elevation motion RAO [m/m]
RAO <sub>Inner</sub>	Inner Body Heave motion RAO with Main Body [m/m]
RAO* <sub>Inner</sub>	Inner Body Heave motion RAO itself [m/m]
R <sub>ext</sub>	Main Body external radius [m]
R <sub>int</sub>	Main Body internal radius [m]
RMS	Root square mean

Su	Space between bodies [m]
S <sub>R</sub>	Response spectrum [m <sup>2</sup> .s]
S <sub>w</sub>	Rea or wave spectrum [m <sup>2</sup> .s]
T <sub>p</sub>	Peak period [s]
WHL	Wind heeling moment curve

## ACKNOWLEDGMENTS

The authors are indebted to the Department of Naval Architecture and Ocean Engineering and the TPN (Numerical Towing Tank) Laboratory of the University of São Paulo, and to Petrobras. The Department of Naval Architecture provided the trial basin for the experimental tests and the TPN Laboratory provided computer facilities and software. Petrobras provided the platform models.

## REFERENCES

- IMO – International Maritime Organization (1997). "MARPOL 73/78 : articles, protocols, annexes, unified interpretations of the International Convention for the Prevention of Pollution from Ships, 1973, as modified by the protocol of 1978 relating thereto", London.
- Malta, E. B. et al. (2004) "Conceptual design of Itapoa Platform", ISODC 2004.
- Wamit, Inc. (2003). "WAMIT®, User Manual, Versions 6.2, 6.2PC, 6.2S, 6.2S-PC".
- Tecgraf, Inc. (2002). "SSTAB® User Manual – Version 2.43 – Floating Systems Stability and Ballast Control" (in Portuguese), Pontificia Universidade Católica do Rio de Janeiro, Rio de Janeiro.
- American Bureau of Shipping (2006). "ABS Guide for Building and Classing - Mobile Offshore Drilling Units".
- Aranha, J. A. P. & Fernandes A. C. (1994). "On the Second Order Slow Drift Force Spectrum of a Floating Body", Applied Ocean Research – 1994.
- Martins, M. R.; Brinati, H. L.; Andrade, B. L. R. (1997). "A Comparative Study of the Conventional and Taut-Leg Mooring System", Proceedings of 1997 International Conference Offshore Mechanics and Arctic Engineering – OMAE 1997. Yokohama, Japan.
- Andrade, B. L. R.; Martins, M.R.; Brinati, H. L. (1997). "A Synthesis Procedure of Mooring System to Reduce Costs and Simplify the Underwater Layout", Proceedings of the Seventh International Offshore and Polar Engineering Conference – ISOPE 1997. Honolulu, Hawaii, USA.
- DNV - Det Norske Veritas (1989). "POSMOR - Position Mooring".
- Poldervaart L. & Pollack J. (2002). "A Dry Tree FPSO Unit for Brazilian Waters", Offshore Technology Conference – OTC 2002, Houston, Texas USA.
- Torres, F. (2007) "Study of Numerical Modeling of Moonpool as Minimization Device of Monocolumn

- Hull*" (in Portuguese), Master Thesis, University of São Paulo, São Paulo, Brazil.
12. Malta, E. B. et al. (2006) "*Numerical Moonpool Modeling*", Proceedings of 2006 International Conference Offshore Mechanics and Arctic Engineering - OMAE2006. Hamburg, Germany.
  13. Cueva, M. et al. (2005) "*Development of Monocolumn Type Deepwater System for GoM - MonoBR*", Proceedings of 2005 International Conference Offshore Mechanics and Arctic Engineering - OMAE2006. Halkidiki, Greece.
  14. Thiagarajan, K. P. & Troesch, A. W. (1998) "*Effects of Appendages and Small Currents on the Hydrodynamic Heave Damping of TLP Columns*", Journal of Offshore Mechanics and Arctic Engineering, ASME 120, 37-42.
  15. Tao, L. & Cai, S. (2004) "*Heave Motion Suppression of a Spar with a Heave Plate*", Ocean Engineering 31 (5-6), 669-692.



## ANNEX A

**Table 1 - Natural periods - Heave motion**

Setup	Nat. Period Main Body [s]	Nat. Period Internal Body [s]
SS1	17.56	-
CI1	-	9.75
SS2	17.45	9.19

**Table 2 - Natural periods - Pitch motion**

Setup	Nat. Period Main Body [s]	Nat. Period Internal Body [s]
SS1	22.49	-
CI1	-	11.06
SS2	22.38	-

**Table 3 - Wave conditions in the Campos Basin**

Sector	1 year		10 year		100 year	
	Tp [s]	Hs [m]	Tp [s]	Hs [m]	Tp [s]	Hs [m]
N	8.81	4.44	9.20	4.74	9.58	5.01
NE	9.13	4.55	9.47	4.88	9.77	5.17
E	9.35	3.72	9.90	4.34	10.40	4.87
SE	10.90	4.81	10.28	5.72	11.63	6.53
S	12.65	5.14	13.54	6.19	14.35	7.10
SW	13.93	6.37	14.78	7.16	15.55	7.84
W	7.91	3.21	8.22	3.57	8.51	3.88
NW	7.91	3.21	8.22	3.57	8.51	3.88

**Table 4 - Wind conditions in the Campos Basin**

Sector	Wind Velocity [m/s]		
	1 year	10 year	100 year
N	17.76	23.22	28.54
NE	18.64	23.91	29.11
E	15.18	20.42	25.57
SE	15.76	21.95	28.05
S	17.52	24.43	31.24
SW	17.31	24.50	31.58
W	16.17	24.08	31.88
NW	13.50	19.29	25.00

**Table 5 - Current conditions in the Campos Basin**

Sector	Current Velocity [m/s]		
	1 year	10 year	100 year
N	1.47	1.76	2.06
NE	1.47	1.70	1.89
E	0.81	0.94	1.04
SE	0.97	1.13	1.26
S	1.12	1.34	1.54
SW	0.81	0.93	1.03
W	0.80	0.97	1.13
NW	1.41	1.62	1.79

Table 6 - Main features of Main Body

Case Id	Loading Condition	Displac. [m³]	Draft [m]	GM [m]	Heave Period [s]	Pitch Period [s]	Oil Storage [BBL]	Inertia [t.m²]	Structural Mass [t]
C01	LC1	146026	26.50	4.96	17.43	37.93	0	1.94E+08	19926
	LC2			11.92		24.04	200775	1.88E+08	
	LC3	192445	38.50	11.89	20.01	23.12	244232	2.28E+08	
	LC4			9.34		26.18	803100	2.30E+08	
C02	LC1	158023	22.00	1.59	16.77	59.50	0	1.65E+08	17640
	LC2			6.43		28.63	204276	1.55E+08	
	LC3	212276	34.00	6.12	19.44	27.48	605702	1.83E+08	
	LC4			3.40		36.98	817103	1.84E+08	
C03	LC1	150535	24.00	1.13	17.14	72.61	0	1.67E+08	17731
	LC2			7.05		27.99	200862	1.55E+08	
	LC3	200035	36.00	7.17	19.76	26.26	567121	1.84E+08	
	LC4			4.30		34.06	803447	1.86E+08	

Table 7 – Main features of Inner Body

Case Id	External Diameter [m]	Draft [m]	Displac. [t]	Structural Mass [t]	Heave Period [s]	Ballast [t]
C01	56.00	30.13	26650	2031	9.88	20000
C02	22.00	26.33	8902	683	9.29	3600
C03	34.00	22.92	10703	1084	8.92	5000

Table 8 - Stability results

	Intact Condition Analyses				Damaged Condition Analyses			
	ABS Rules	Case C01	Case C02	Case C03	ABS Rules	Case C01	Case C02	Case C03
		LC1	LC1	LC1		LC4	LC4	LC4
Corrected Transversal GM [m]	> 1.0	5.04	1.44	1.37	-	9.55	6.06	5.74
Area Ratio	> 1.3	8.11	9.31	7.29	-	7.29	2.22	2.74
Stability Range [degree]	-	29.11	35.93	32.55	> 7.0	12.14	4.47	7.24
GZ / WHL max	-	15.85	17.66	15.26	> 2.0	12.32	4.29	5.54
Status	-	ok	ok	ok	-	ok	rejected	ok

Table 9 – Significant height of Heave motion [m] – Main Body

Case Id	Loading Condition	Sea 1	Sea 2	Sea 3
C01	LC2	9.47	12.85	16.49
	LC3	8.77	12.40	15.80
C03	LC2	5.00	7.63	13.71
	LC3	6.66	10.15	13.77

Table 10 – Significant height of Pitch motion [degree] – Main Body

Case Id	Loading Condition	Sea 1	Sea 2	Sea 3
C01	LC2	1.65	1.78	1.95
	LC3	0.84	1.89	3.53
C03	LC2	3.99	4.29	4.51
	LC3	0.83	1.05	2.09

**Table 11 – Significant height of Heave motion [m] – Inner Body**

Case Id	Loading Condition	Sea 1	Sea 2	Sea 3
C01	LC2	4.66	4.87	5.18
	LC3	4.31	5.30	5.73
C03	LC2	2.89	3.05	3.21
	LC3	2.51	2.80	2.96

**Table 12 - Significant height of Heave motion [m] - Including viscous damping - Main Body**

Viscous Damping	Loading Condition	Sea 1	Sea 2	Sea 3
$\zeta=2\%$	LC2	3.07	4.55	6.12
	LC3	3.70	5.71	7.80
$\zeta=4\%$	LC2	2.43	3.48	4.64
	LC3	2.87	4.40	6.01
$\zeta=6\%$	LC2	2.10	2.91	3.84
	LC3	2.39	3.63	4.96

**Table 13 - Significant height of Pitch motion [degree] - Including viscous damping - Main Body**

Viscous Damping	Loading Condition	Sea 1	Sea 2	Sea 3
$\zeta=2\%$	LC2	3.97	4.27	4.48
	LC3	0.83	0.90	0.97
$\zeta=4\%$	LC2	3.97	4.27	4.48
	LC3	0.83	0.90	0.97
$\zeta=6\%$	LC2	3.97	4.27	4.48
	LC3	0.83	0.90	0.97

**Table 14 - Significant height of Heave motion [m] - Including viscous damping - Inner Body**

Viscous Damping	Loading Condition	Sea 1	Sea 2	Sea 3
$\zeta=2\%$	LC2	1.17	1.31	1.44
	LC3	0.81	1.00	1.18
$\zeta=4\%$	LC2	1.15	1.21	1.40
	LC3	0.78	0.95	1.10
$\zeta=6\%$	LC2	1.13	1.26	1.38
	LC3	0.77	0.93	1.07

**Table 15 – Significant height of relative motion between the bodies [m]**

Viscous Damping	Loading Condition	Sea 1	Sea 2	Sea 3
$\zeta=2\%$	LC2	3.45	5.06	6.77
	LC3	4.48	6.80	9.19
$\zeta=4\%$	LC2	2.79	3.96	5.19
	LC3	3.41	5.25	7.15
$\zeta=6\%$	LC2	2.46	3.35	4.37
	LC3	2.85	4.35	5.93